JOURNAL OF MATERIALS SCIENCE **34** (1999) 2733–2739

Characterization of polyaniline by cyclic voltammetry and UV-Vis absorption spectroscopy

S. PRUNEANU
Institute of Isotopic and Molecular Technology, P.O. Box 700, Cluj-Napoca 3400, Romania
E-mail: stelep@oc1.itim-cj.ro

E. VERESS
Institute of Chemistry, Cluj-Napoca 3400, Romania

I. MARIAN, L. ONICIU
University of Cluj, Faculty of Chemistry, Arany Janos 11, Cluj-Napoca 3400, Romania

Characterization of polyaniline (PANI) by electrochemical and spectroscopic techniques are presented. The electrochemical investigation reveals the influence of the dopant acid on the kinetic parameters of polyaniline films: exchange current density (I_0) and the cathodic transfer coefficient (α_c). UV-Vis spectra of thin films of polyaniline in *N*-metil pyrrolidine solutions indicate the increase of the absorbance with the number of deposition cycles, *N*. The inhibition of polymer degradation in thick films was confirmed by these spectra.

1. Introduction

Polyaniline (PANI) is an important conducting polymer because of its good stability in air, both in the isolating form (emeraldine base) and in the conducting form (emeraldine salt). It can be electrochemically prepared by polymerizing aniline in acidic aqueous solutions under a constant voltage [1] or by cyclic voltammetry [2, 3].

The formation of quality PANI films is strongly influenced by the removal of unreacted oxidized species [4]. These species can react with water, leading to polymer degradation (hydrolysis). The deposition of PANI by cyclic voltammetry has the advantage of a short exposure time at anodic potential and the reduction of the unreacted oxidized species during the cathodic scan. As a result, the incorporation of hydrolysis products in the PANI deposits decreases and a more conductive and thicker film can be produced.

In this paper we focused on the electrochemical and optical properties of polyaniline, prepared by cyclic voltammetry. We have determined the kinetic parameters for PANI films, prepared with two organic acids (chloroacetic and trichloroacetic) and the results were compared with those obtained with $HClO_4$.

UV-Vis absorption spectra of PANI solutions in *N*-metil pyrrolidine (NMP) evidence that the degradation pf PANI is higher in the early stage of deposition. This fact was characteristic for all the three dopant acids used during the electropolymerization process.

2. Experimental

The electrochemical synthesis and characterization of polyaniline (PANI) were carried out at room temperature, in a standard three electrode cell. The working electrode was a Pt disc (area = 0.005 cm^2) and the counter electrode was a Pt foil (area = 0.36 cm^2). As reference electrode we used a saturated calomel electrode (SCE). Prior to each electrochemical synthesis, the working electrode was carefully polished with abrasive paper and then washed with distilled water. Aniline was used after distillation while other chemicals were used as received. Potentiostatic control was provided by a Radelkis potentiostat connected with the cell and a Kipp & Zonnen X-Y recorder.

PANI films were deposited from 1 M acidic aqueous media containing 0.2 M aniline, by voltammetric sweep between −0.2 V and 0.9 V/SCE, at 160 mV s^{-1}. The sweep was stopped after 30 cycles at −0.2 V/SCE and the working electrode covered by PANI film was removed from the monomer solution and washed thoroughly with distilled water.

Voltammetric studies were performed in 1 M acidic aqueous solutions, using different acids: perchloric acid ($HClO_4$), trichloroacetic acid ($C_2HCl_3O_2$) and chloroacetic acid ($C_2H_3ClO_2$).

The electronic structure of PANI films was determined from UV-Vis absorption spectra of PANI solutions in *N*-metil pyrrolidine on a Ultrospect 3 LKB spectrophotometer.

3. Results and discussion

Fig. 1 shows cyclic voltammograms (CVs) of PANI-$HClO_4$ films, recorded at different sweep rate (from 10 to 200 mV s^{-1}), in 1 M $HClO_4$ aqueous solution. There are three redox pairs, with oxidation peaks at 0.125 V (A), 0.5 V (B) and 0.7 V/SCE (C). For the first redox pair AA′, the increase of the sweep rate doesn't influence the position of the two peak potentials. Instead,

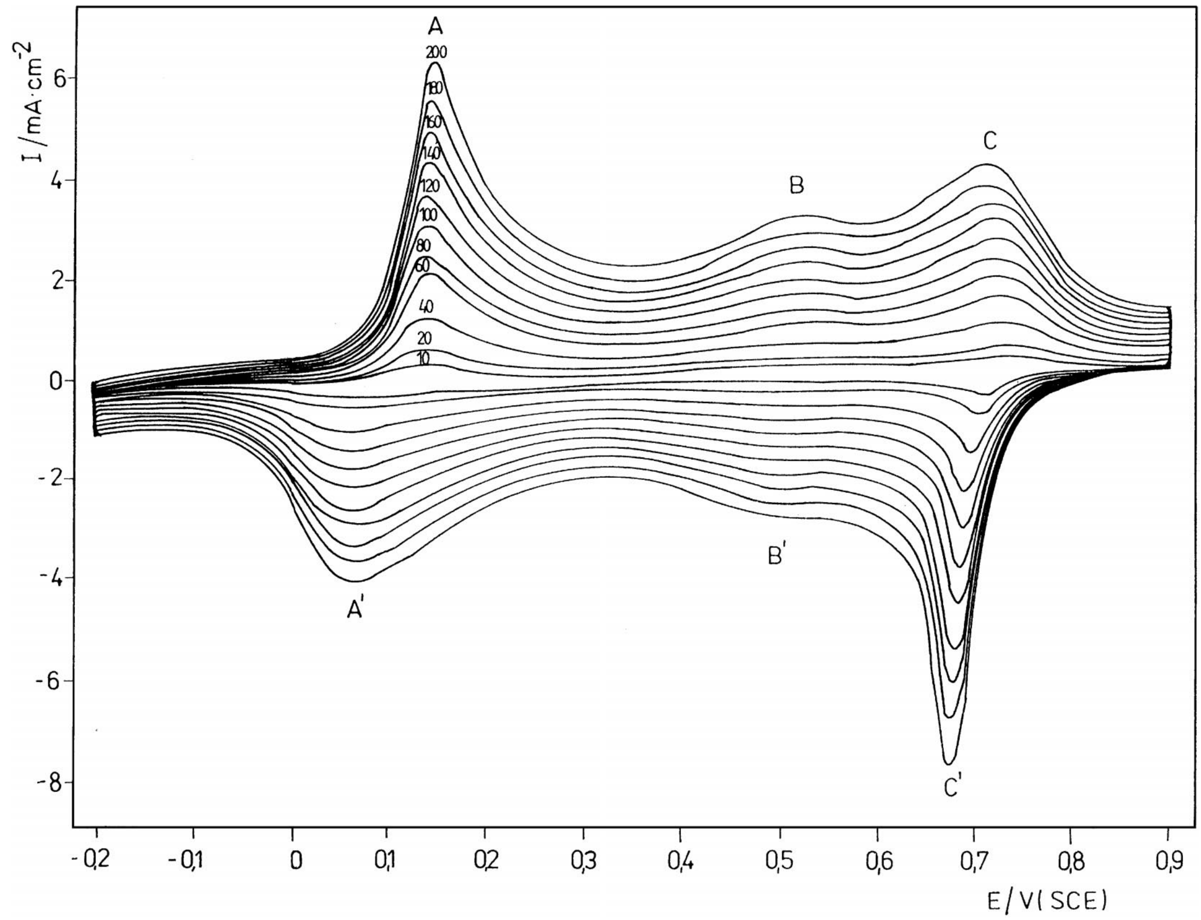

Figure 1 Cyclic voltammograms of PANI-$HClO_4$ film, recorded at different sweep rate (from 10 to 200 mV s^{-1}), in 1 M $HClO_4$ aqueous solution.

for the third redox pair CC′, the anodic and cathodic peak potential are shifted towards lower potential, by increasing the sweep rate. Also, the peak potential separation increases from 30 mV ($V = 10$ mV s^{-1}) up to 40 mV ($V = 200$ mV s^{-1}).

The second redox pair BB′ is almost undistinguishable at low sweep rate ($V = 10$ mV s^{-1}), but gradually increases with it. According to the literature, the oxidation peaks A and C correspond to the changes in the oxidation state of the PANI films. Snauwaert *et al.* [5] have evidenced, by X-ray photoelectron spectroscopy, that the ratio between the amine and imine content is function of the electrochemical potential. At 0.15 V/SCE the imine concentration is about 25% (protoemeraldine) and gradually increases to 50% (emeraldine) at 0.6 V/SCE and then up to 80% (nigraniline) at 0.8 V/SCE. The amine concentration is higher at low potential (75% at 0.15 V/SCE) and decreases to 20%, at 0.8 V/SCE.

So, the first peak A corresponds to the first step of oxidation of neutral PANI, and the third peak C corresponds to the further oxidation of PANI, from emeraldine to nigraniline. The middle pair BB′ has been attributed either to the presence of ortho-coupled polymers [6] or to the degradation of PANI (soluble species such as benzoquinone and hydroquinone) [7].

In Fig. 2 are shown voltammograms of PANI in 1 M trichloroacetic acid, recorded at different sweep rates, from 10 to 200 mV s^{-1}. The first oxidation peak (A) appears at about 0.18 V/SCE and the third oxidation peak (C) appears at about 0.55 V/SCE. The middle peak B is not distinct on the oxidation wave, only on the reduction wave (B′).

For the first redox pair AA′, the increase of the sweep rate shifts the position of the two peak potentials towards higher potentials. The third redox pair CC′ is characterized by a constant value for the anodic peak potential and by a gradually shift of the cathodic peak potential towards lower potentials, with the sweep rate. The third peak C exhibits a very broad oxidation wave comparing with the first peak, A. This indicates that the charge transfer takes place more difficult for the second step of oxidation of PANI than for the first step of oxidation.

Fig. 3 shows CVs of PANI in 1M chloroacetic acid, recorded at different sweep rates. All voltammograms are characterized by a single redox pair AA, with broad anodic and cathodic waves.

The anodic peak potentials shifts towards higher potentials while the cathodic peak potentials shifts towards lower potentials, with the sweep rate.

From the cyclic voltammograms represented in Figs 1–3 we can observe that the oxidation and reduction potentials are different for each dopant acid. This fact was attributed to the electrostatic interaction of the dopant with the chemically flexible -NH- group of the polymer [8].

The kinetic of the electron transfer process depends on the exchange current density (I_0) and the anodic and cathodic transfer coefficients (α_A, α_C). The values

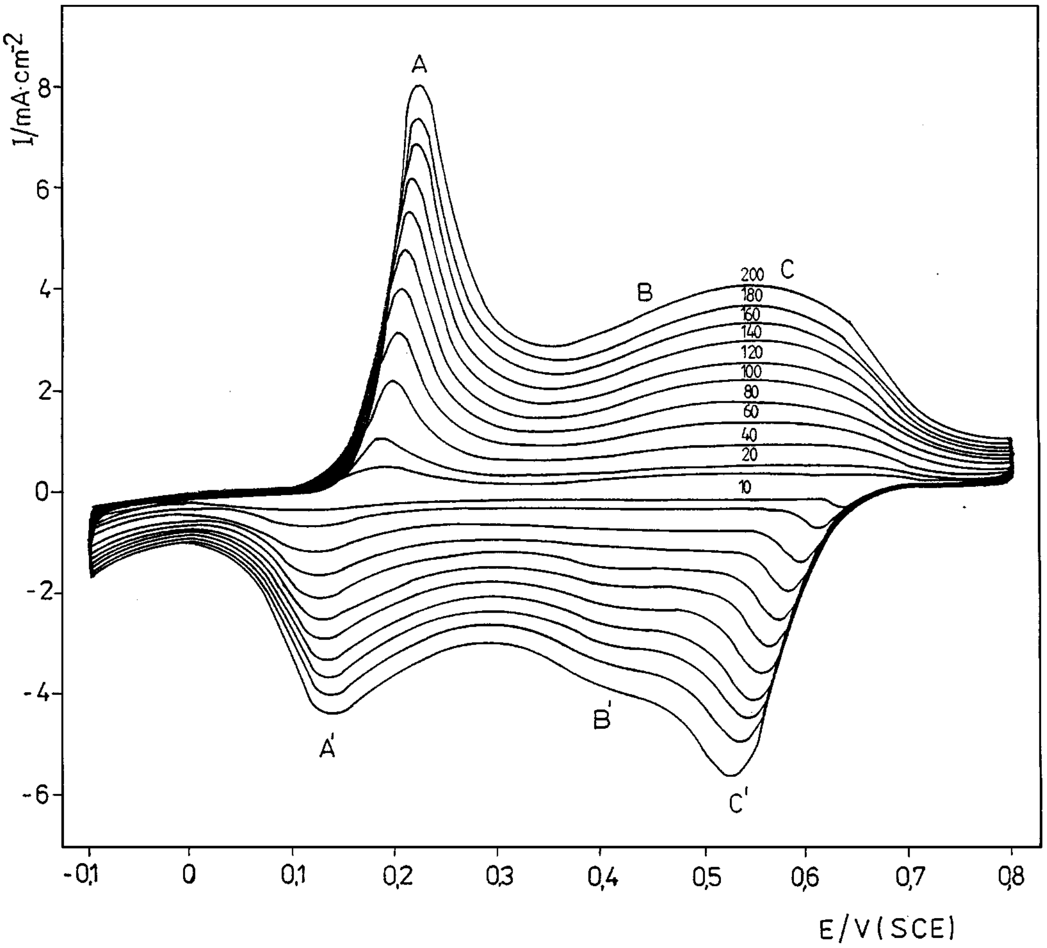

Figure 2 Cyclic voltammograms of PANI-$C_2HCl_3O_2$ film, recorded at different sweep rate (from 10 to 200 mV s^{-1}), in 1 M $C_2HCl_3O_2$ aqueous solution.

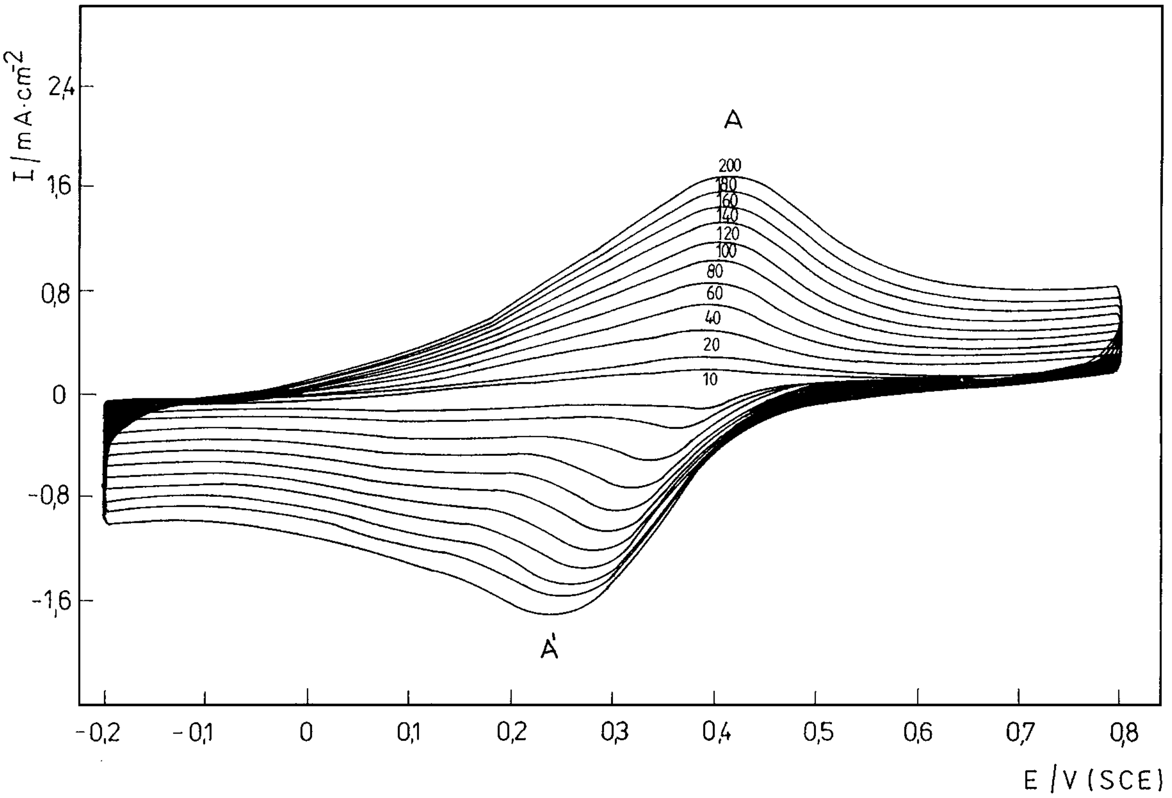

Figure 3 Cyclic voltammograms of PANI-$C_2H_3ClO_2$ film, recorded at different sweep rate (from 10 to 200 mV s^{-1}), in 1 M $C_2H_3ClO_2$ aqueous solution.

of these parameters can be obtained from Tafel Equations 1 and 2 [9]:

$$\log(I) = \log(I_0) + \frac{\alpha_A nF}{2.3nF}(E - E_e) \quad \text{anodic process} \quad (1)$$

$$\log(-I) = \log(I_0) - \frac{\alpha_C nF}{2.3RT}(E - E_e) \quad \text{cathodic process} \quad (2)$$

where $E - E_e$ is the overpotential and n is the number of electrons involved in the redox process, in our case $n = 1$.

The Tafel approximation is generally used for $|E - E_e| \geq 100/n$ mV. The exchange current density's value, I_0, is obtained from the intercept of $\log|I|$ versus $E - E_e$ plots, while the values of α_A, α_C are obtained from the slopes of these plots.

Tafel curves for PANI-$HClO_4$ films are shown in Fig. 4. We observed that for the anodic process, Tafel plot rises abruptly and then reaches a plateau (in the range of 60 mV to 80 mV/SCE).

This fact indicates that the first step of oxidation of PANI is very fast and takes place very close to the equilibrium potential ($|E - E_e| = 60$ mV). For the cathodic process, Tafel plot rises slowly and also reaches a plateau (for $|E - E_e| > 80$ mV).

Since Tafel equations apply for $|E - E_e| \geq 100/n$ mV, we have determined the kinetic parameters only for the cathodic process and they are listed in Table I.

TABLE I Kinetic parameters derived from Tafel equations, for PANI films prepared with various acids

Sample	I_0 (mA/cm^2)	α_C
PANI-$HClO_4$	0.048	0.09
PANI-$C_2H_3ClO_2$	0.036	0.1
PANI-$C_2HCl_3O_2$	0.03	0.29

Tafel curves for PANI-$C_2HCl_3O_2$ films are represented in Fig. 5.

They are similar with those shown in Fig. 4, for PANI-$HClO_4$. The anodic plot rises abruptly (in the range of 20 to 90 mV/SCE) while the cathodic plot rises slowly. So, the first step of oxidation of PANI-$C_2HCl_3O_2$ also takes place very quickly. The kinetic parameters obtained for the cathodic process are listed in Table I.

Tafel curves for PANI-$C_2H_3ClO_2$ (Fig. 6) are different comparing with those represented in Figs 4 and 5. Both the anodic and cathodic plots rise slowly and reach a plateau, for $|E - E_e| > 80$ mV.

In Table I are listed the values of the kinetic parameters I_0, α_C for PANI films prepared with three different acids: perchloric, $HClO_4$, trichloroacetic, $C_2HCl_3O_2$ and chloroacetic, $C_2H_3ClO_2$. The highest value of I_0 was obtained for PANI-$HClO_4$ and the lowest value for PANI-$C_2HCl_3O_2$. Since the cation was the same for all the electrolytes used (H^+), these differences arise from the different structure and molecular weight of the anions. The higher the molecular weight of the anions, the smaller the value of I_0.

4. Electronic structure

The best organic solvent found for emeraldine base is N-metil pyrrolidine (NMP). PANI salts doped by the two organic acids ($C_2H_3ClO_2$ and $C_2HCl_3O_2$) and $HClO_4$ are also soluble in NMP. A large excess of NMP leads to the deprotonation of the salts to emeraldine base. This is due to the C=O groups in NMP that forms hydrogen bonds with the dopant acid and inhibits the doping process [10]. The re-protonation of the emeraldine base can be obtained by adding an excess of the doping acid (acid/emeraldine monomer unit ratio greater than 10) [11]. The colour of the solution turns from blue to green, indicating the protonation of the emeraldine base.

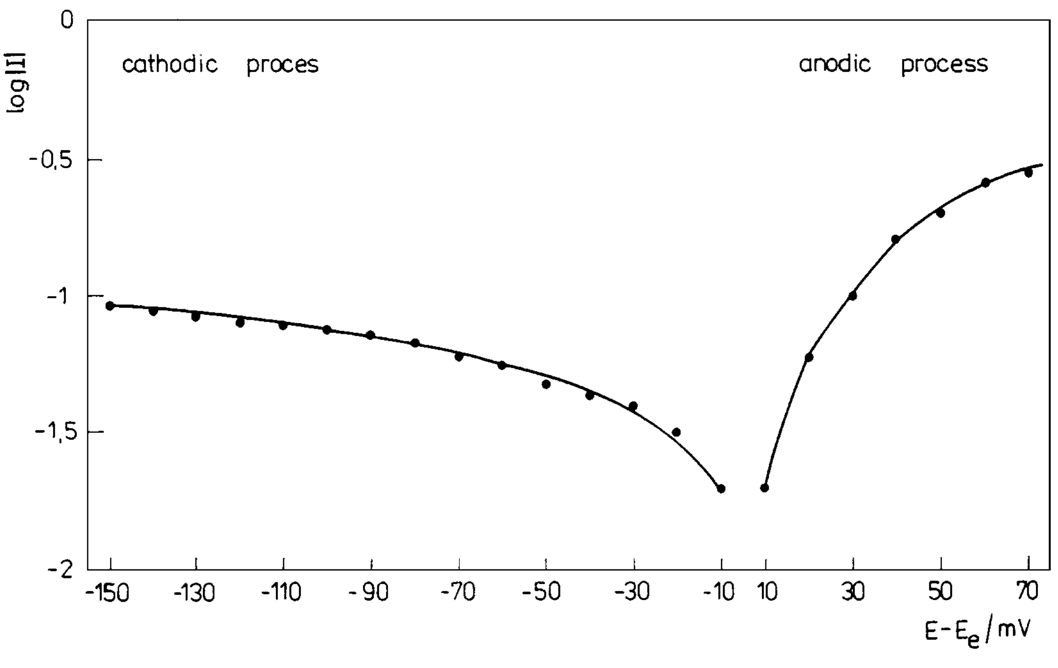

Figure 4 Tafel curves for PANI-$HClO_4$ film.

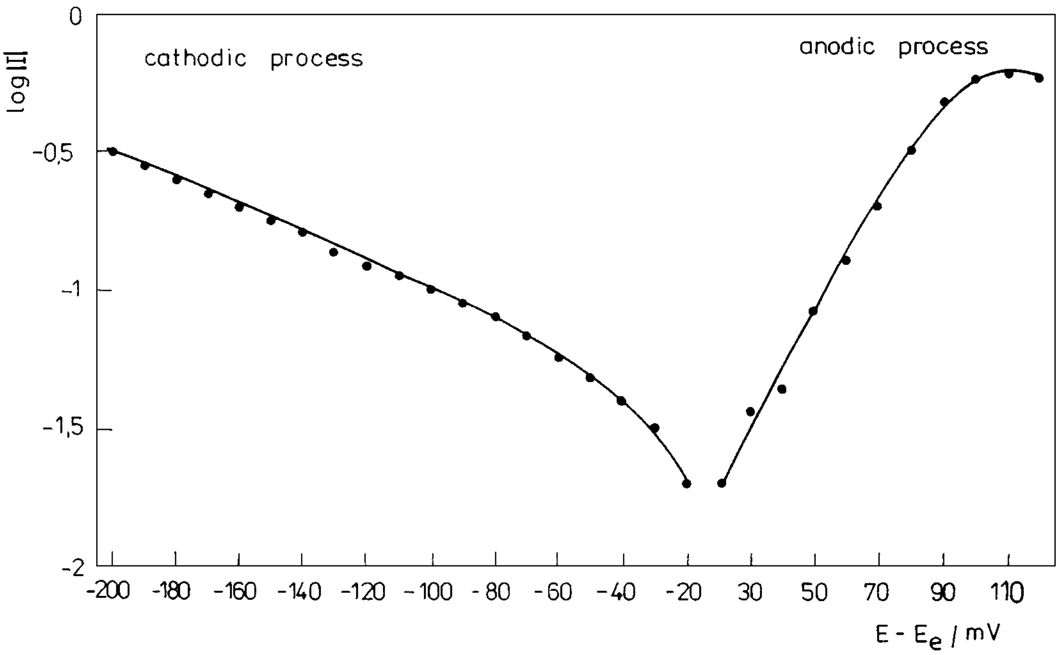

Figure 5 Tafel curves for PANI-$C_2HCl_3O_2$ film.

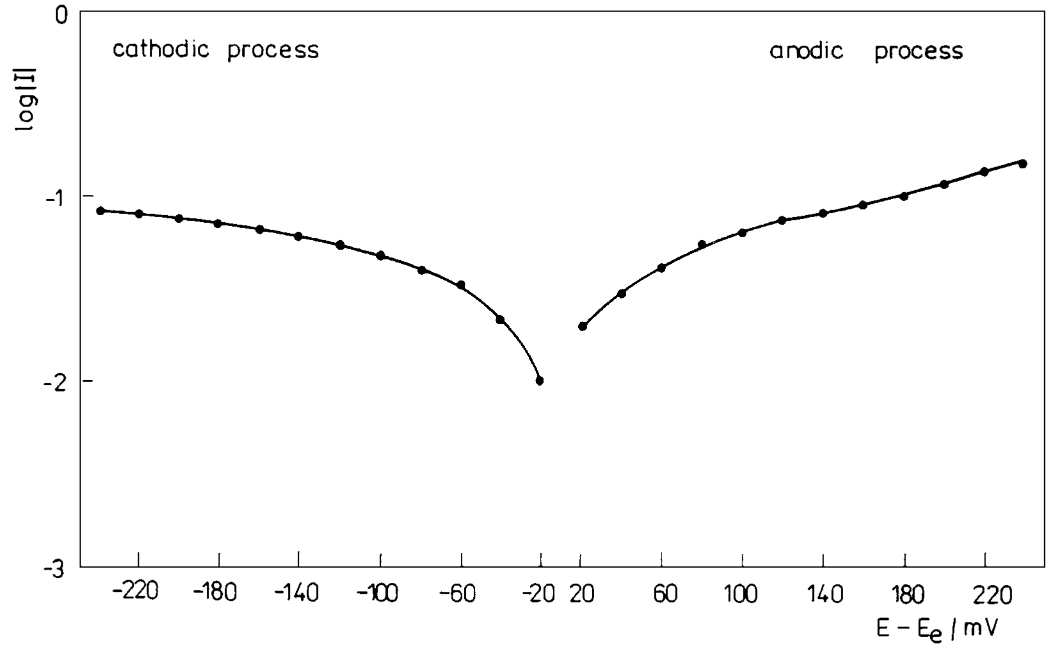

Figure 6 Tafel curves for Pani-$C_2H_3ClO_2$ film.

PANI-$HClO_4$ electronic structure, for various film thicknesses (expressed in terms of the number of deposition cycles, N) is represented in Fig. 7.

The spectra are characteristic for the emeraldine base formed upon the deprotonation action of NMP on the PANI salt. The spectra are dominated by two absorption peaks at 320 and 610 nm, respectively. The 320 nm band is often assigned to a $\pi - \pi^*$ transition in the benzoid structure [12, 13]. The absorption in the visible range, at 610 nm, is ascribed to exciton formation in the quinoid rings [14]. This absorption gives rise to a blue coloration of the PANI-NMP solution. The position of the 610 nm absorption band is a little shifted with film thickness.

From these spectra we can observe that the absorbance doesn't increase linearly with the number of deposition cycles, N (it is higher for $N > 40$). This fact indicates that the thickness of PANI-$HClO_4$ film doesn't increase linearly with N. These results are consistent with those of Zhang *et al.* [10], who have studied the extent of polymer degradation during electropolymerization process. They evidenced that the degardation of PANI-$HClO_4$ is higher in the early stage of deposition ($N \leq 20$ cycles) and then this process decreases and reaches a steady state, for $N \geq 40$ cycles.

Since aniline is a stronger nucleophile than water, the growth of the PANI film dominates over hydrolysis (degradation). This will lead to an autocatalytic growth

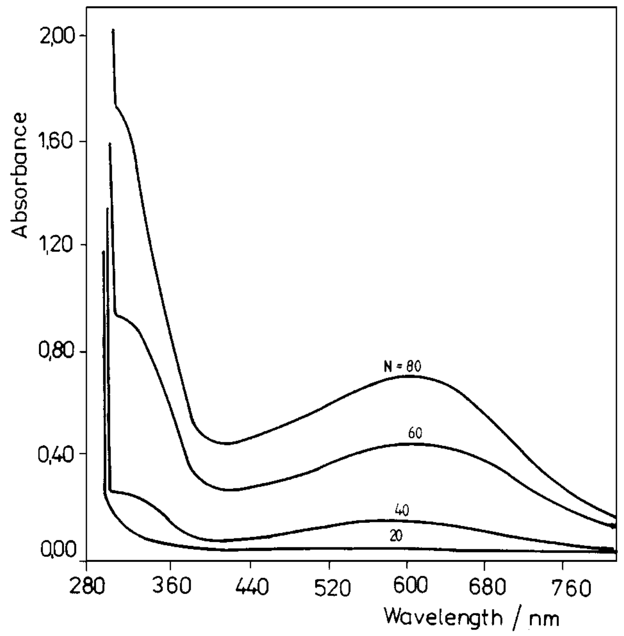

Figure 7 UV-Vis absorption spectra of PANI-$HClO_4$ deposits of different thicknesses, in N-metil pyrrolidine. The thickness is expressed in terms of the number of deposition cycles, N.

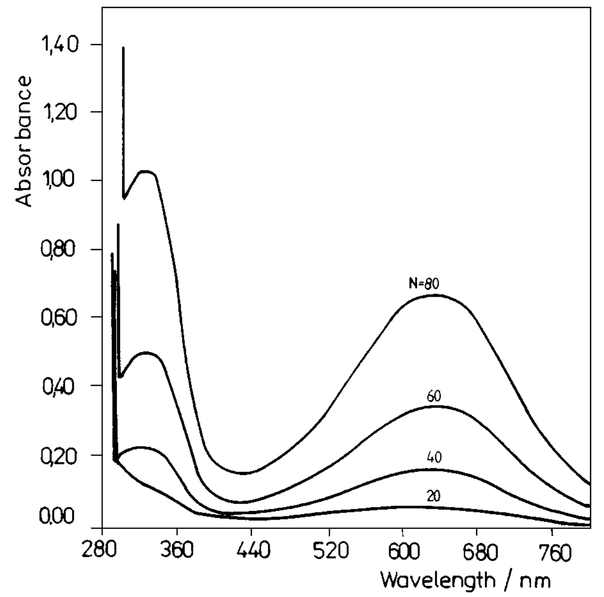

Figure 8 UV-Vis absorption spectra of PANI-$C_2HCl_3O_2$ deposits of different thicknesses, in N-metil pyrrolidine. The thickness is expressed in terms of the number of deposition cycles, N.

of the polymer. However, in the early stage of deposition of PANI (when is insufficient PANI for autocatalitic growth) the cations formed react with water, leading to the degradation of PANI. This process diminishes after a number of deposition cycles.

Shown in Fig. 8 are the spectra of PANI-$C_2HCl_3O_2$ in NMP solutions, for various film thicknesses (expressed in terms of the number of deposition cycles, N).

Similar to the spectra obtained for PANI-$HClO_4$, there are spectral features at 330 and 630 nm, characteristic for the emeraldine base. Note that, in this case, the 330 nm absorption band is well defined and there is no shift in the position of the 630 nm absorption band, with the film thickness. The increase of the absorbance

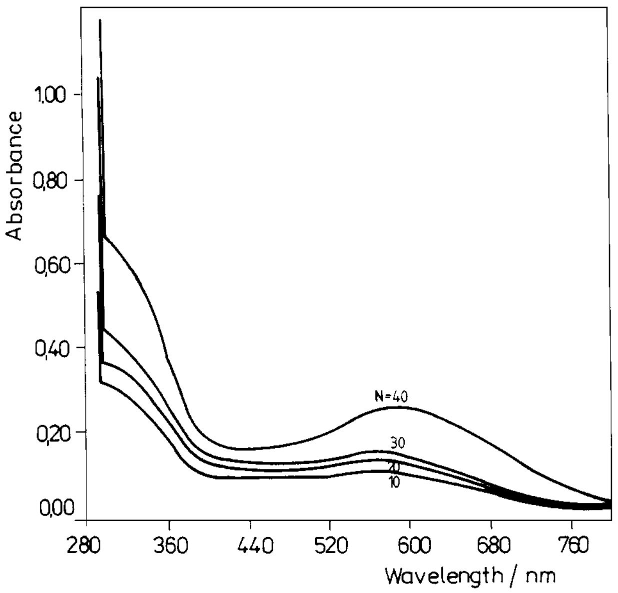

Figure 9 UV-Vis absorption spectra of PANI-$C_2H_3ClO_2$ deposits of different thicknesses, in N-metil pyrrolidine. The thickness is expressed in terms of the number of deposition cycles, N.

for $N > 40$ cycles is consistent with the inhibition of polymer degradation in thick films. The radical cations responsible for both polymerization and degradation become more selective and facilitate the polymerization process.

For PANI films deposited from $C_2H_3ClO_2$ at $N \leq 30$ cycles (Fig. 9), the absorption band from the visible range appears around 570 nm. This band shifts towards 600 nm for $N = 40$ cycles.

In the ultraviolet region the absorption band is not well defined and appears as a shoulder. The strong absorption of the solvent (NMP) in this region makes difficult the appearance of this band. The pronounced degradation of PANI, that occurs in the early stage of deposition ($N \leq 30$ cycles), diminishes after a higher number of deposition cycles ($N > 40$ cycles).

5. Conclusions

The characteristics of polyaniline doped by two organic acids (chloroacetic and trichloroacetic) have been investigated and compared with those of $HClO_4$ doped salt. The redox properties of PANI deposits are strongly influenced by the dopant acid. The oxidation and reduction potentials are different for each acid and this fact can be attributed to the electrostatic interaction of the dopant with the chemically flexible -NH- group of the polymer. The values of the kinetic parametrs I_0, α_C also depends on the type of acid used during the electropolymerization process.

UV-Vis absorption spectra of thin solution film of PANI in N-metil pyrrolidine indicate the inhibition of polymer degradation in thick films and this fact was characteristic for all the three dopant acids.

References

1. D. M. MOHILNER, R. N. ADAMS and W. J. ARGERSINGER, JR., *J. Amer. Chem. Soc.* **84** (1962) 3618.

2. E. M. GENIES, A. A. SYED and C. TSINTAVIS, *Mol. Cryst. Liq. Cryst.* **121** (1985) 181.
3. A. KITANI, J. IZUMI, J. YANO, Y. HIROMOTO and K. SASAKI, *Bull. Chem. Soc. Jpn.* **57** (1984) 2254.
4. C. Q. CUI, L. H. ONG, T. C. TAN and JIM Y. LEE, *Synth. Metals* **58** (1993) 147.
5. P. SNAUWAERT, R. LAZZARONI, J. RIGA, J. VERBIST and D. GONBEAU, in "Electronic Properties of Conjugated polymers III, Springer Series in Solid State Sciences," Vol. 91, edited by H. Kuzmany, M. Mehring and S. Roth (Springer, Berlin, 1989) pp. 301–304.
6. R. L. HAND and R. F. NELSON, *J. Amer. Chem. Soc.* **96** (1974) 850.
7. V. B. SHIM, M. S. WON and S. M. PARK, *J. Electrochem. Soc.* **137** (1990) 538.
8. D. C. TRIVEDI and S. K. DHAWAN, *Synth. Metals* **58** (1993) 309.
9. R. GREEF, R. PEAT, L. M. PETER, D. PLETCHER and J. ROBINSON, "Instrumental Methods in Electrochemistry" (Ellis Horwood, Chichester, 1980) p. 25.
10. S. A. CHEN and H. T. LEE, *Macromolecules* **26** (1993) 3354.
11. K. G. NEOH, E. T. KANG and K. L. TAN, *Polymer* **33** (1992) 2292.
12. P. ZACH, *J. Polym. Sci.* **10** (1972) 2379.
13. C. N. R. RAO, "Ultra-Violet and Visible Spectroscopy," 2nd ed. (Butterworth, Guildford, 1967).
14. A. P. MONKMAN, in "Conjugated Polymeric Materials, Nato ASI Series E: Applied Sciences," Vol. 182, edited by J. L. Bredas and R. R. Chance (Kluwer, Dordrecht, The Netherlands, 1990) p. 273.

Received 11 November 1996
and accepted 15 December 1998